J Neurophysiol 112: 951–961, 2014.
First published May 28, 2014; doi:10.1152/jn.00150.2014.

Neural and genetic degeneracy underlies *Caenorhabditis elegans* feeding behavior

Nicholas F. Trojanowski,[1,2,3] Olivia Padovan-Merhar,[1] David M. Raizen,[2] and Christopher Fang-Yen[1,3,4]

[1]*Department of Bioengineering, University of Pennsylvania, Philadelphia, Pennsylvania;* [2]*Department of Neurology, University of Pennsylvania, Philadelphia, Pennsylvania;* [3]*Department of Neuroscience, University of Pennsylvania, Philadelphia, Pennsylvania; and* [4]*Department of Physics, Korea University, Anam-dong, Seongbuk-gu, Seoul, South Korea*

Submitted 20 February 2014; accepted in final form 23 May 2014

Trojanowski NF, Padovan-Merhar O, Raizen DM, Fang-Yen C. Neural and genetic degeneracy underlies *Caenorhabditis elegans* feeding behavior. *J Neurophysiol* 112: 951–961, 2014. First published May 28, 2014; doi:10.1152/jn.00150.2014.—Degenerate networks, in which structurally distinct elements can perform the same function or yield the same output, are ubiquitous in biology. Degeneracy contributes to the robustness and adaptability of networks in varied environmental and evolutionary contexts. However, how degenerate neural networks regulate behavior in vivo is poorly understood, especially at the genetic level. Here, we identify degenerate neural and genetic mechanisms that underlie excitation of the pharynx (feeding organ) in the nematode *Caenorhabditis elegans* using cell-specific optogenetic excitation and inhibition. We show that the pharyngeal neurons MC, M2, M4, and I1 form multiple direct and indirect excitatory pathways in a robust network for control of pharyngeal pumping. I1 excites pumping via MC and M2 in a state-dependent manner. We identify nicotinic and muscarinic receptors through which the pharyngeal network regulates feeding rate. These results identify two different mechanisms by which degeneracy is manifest in a neural circuit in vivo.

behavior; feeding; neural circuits; optogenetics

ALL LIVING SYSTEMS POSSESS mechanisms for maintaining their function in varied internal and external environments. One mechanism that generates this adaptability is degeneracy, the ability of structurally distinct elements to perform the same function or yield the same output under specific conditions (Tononi et al. 1999). Degeneracy is a ubiquitous property of biological systems at all levels of organization (Edelman and Gally 2001) and supports robustness and adaptability by providing the capability to produce a variety of actions, both overlapping and unique, depending on context (Tononi et al. 1999). The degeneracy of a system has been proposed to correlate with its complexity (Edelman and Gally 2001; Tononi et al. 1999). Studies in the crustacean stomatogastric ganglion have demonstrated that even small neural circuits can be highly degenerate; similar functional network performance can be achieved with many different network parameters (Grashow et al. 2010; Gutierrez et al. 2013; Marder and Taylor 2011; Prinz et al. 2004; Rodriguez et al. 2013; Saideman et al. 2007). However, the mechanisms by which different network activity patterns generate similar behaviors in vivo are poorly understood.

Address for reprint requests and other correspondence: D. M. Raizen, Dept. of Neurology, Univ. of Pennsylvania, Philadelphia, PA 19104 (e-mail: raizen@mail.med.upenn.edu).

Here, we investigate degeneracy in the pharyngeal nervous system of the nematode *Caenorhabditis elegans*. The worm feeds on bacteria via rhythmic contractions and relaxations of the pharynx, which trap the bacteria, crush it, and transport it to the intestine (Doncaster 1962; Fig. 1, *A* and *B*). The pharynx has two stereotyped behaviors: *1*) pumping, which is a rhythmic contraction and relaxation of the corpus, anterior isthmus, and terminal bulb; and *2*) isthmus peristalsis, which normally occurs after one out of every three to four pumps and transports food particles from the anterior isthmus to the terminal bulb and intestine.

The pharynx is innervated by a well-mapped pharyngeal nervous system containing 20 identified neurons of 14 types and <60 unique chemical and electric synapses (Albertson and Thomson 1976). The pharyngeal nervous system is synaptically connected to the 282-neuron somatic nervous system by a single pair of gap junctions (Albertson and Thomson 1976).

Pharyngeal pumping requires the neurotransmitter ACh (Alfonso et al. 1993; Avery and Horvitz 1990), which is synthesized by 5 pharyngeal neuron types (Fig. 1, *A* and *C*). By using laser ablation to kill individual neuron classes, Avery and colleagues identified the paired cholinergic MC cells as the only neurons required for rapid feeding (Avery and Horvitz 1989; Raizen et al. 1995). However, ablation of other cholinergic pharyngeal neurons, such as the M2s and M4, only slightly decreases feeding rate (Avery and Horvitz 1989; Raizen et al. 1995), demonstrating that the network that regulates feeding rate is robust. In fact, feeding continues even after ablation of all pharyngeal neurons, albeit in a slow and uncoordinated manner (Avery and Horvitz 1989).

Work with other nematode species suggests that the pharyngeal nervous system is highly evolutionarily adaptable and more functionally complex than the *C. elegans* ablation results alone indicate. The structural connectivity of the pharyngeal nervous system of the nematode *Pristionchus pacificus* has recently been shown to be very similar to that of *C. elegans* (Bumbarger et al. 2013). Although *C. elegans* and *P. pacificus* diverged ~300 million years ago (Dieterich et al. 2008; PiresdaSilva and Sommer 2004) and have different feeding strategies, there is near-perfect homology of pharyngeal neurons between these species (Bumbarger et al. 2013). Strikingly, the morphologies of the neuronal processes are nearly identical, and a remarkable number of connections are conserved (Bumbarger et al. 2013). As in *C. elegans*, M4 ablation in *P. pacificus* causes a mild decrease in feeding rate (Chiang et al. 2006). M2 ablation in the nematode *Panagrolaimus* sp. PS1159

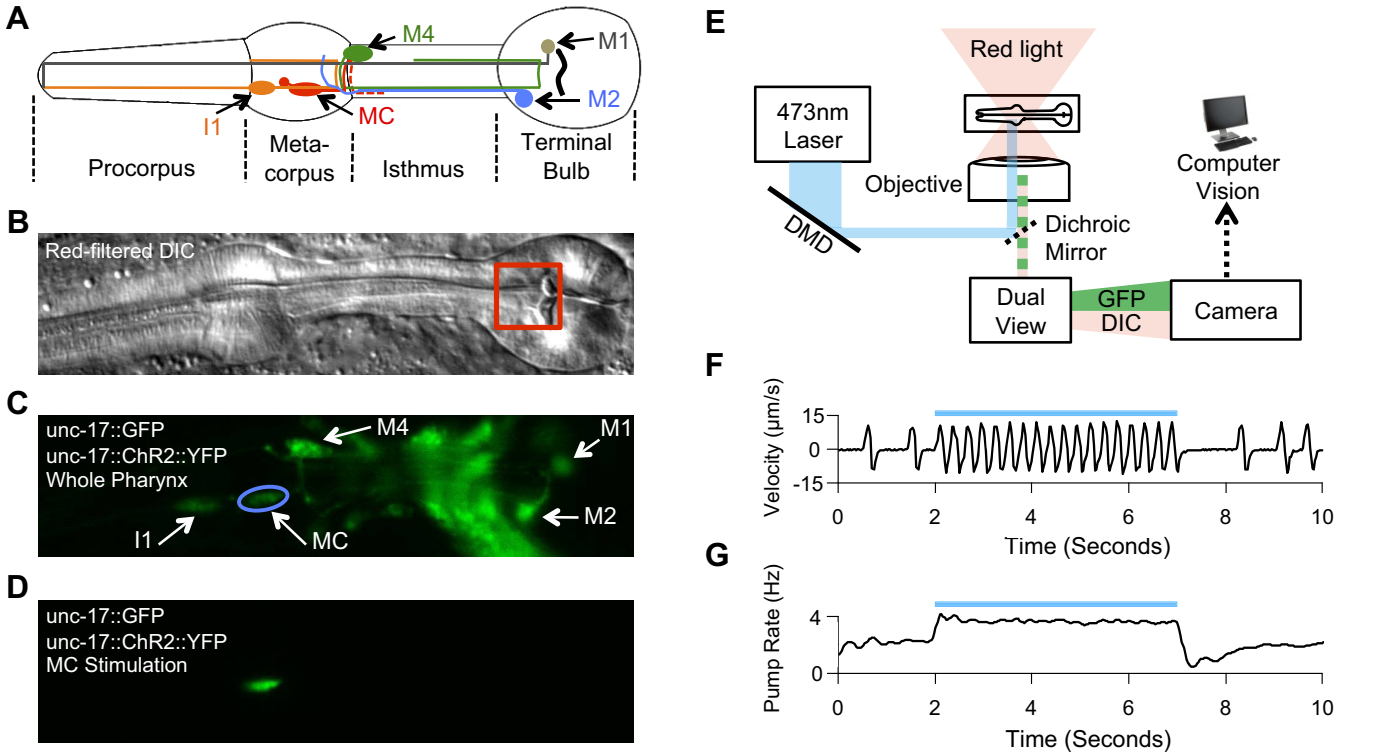

Fig. 1. Optogenetic stimulation of the pharyngeal cholinergic nervous system and machine vision quantification of pumping. *A*: cholinergic pharyngeal neurons. Only 1 of each of the paired I1, MC, and M2 neurons is shown. In *A–D*, anterior is to the left, and ventral is toward the bottom. *B*: differential interference contrast (DIC) image of the pharynx. Red box denotes region used for velocity calculations. *C*: wide-field green fluorescent protein (GFP) fluorescence image of the same field of view as in *B*. The blue circle represents a stimulus region for an MC soma. *D*: GFP fluorescence image of the same field of view as in *B* and *C* during selective illumination of an MC soma. *E*: experimental schematic. A laser beam with 473-nm wavelength is shaped by a digital micromirror device (DMD) and enters a microscope to stimulate selectively neurons of interest expressing either GFP- and yellow fluorescent protein (YFP)-tagged blue-light-sensitive channelrhodopsin-2 (ChR2) or YFP-tagged blue-light-powered proton pump (Mac) from *Leptoshaeria maculans*. Pharyngeal behavior is imaged using a red filter and DIC optics. *F*: velocity from machine vision algorithm during ChR2-mediated stimulation of the MCs. Each peak in the velocity represents a pump. *G*: mean pump rate from 9 intervals of MC excitation in each of 10 worms. In *F* and *G*, the blue bar denotes timing of laser illumination.

also causes a mild decrease in feeding rate (Chiang et al. 2006). Pharyngeal neuron homology has also been observed in nematode species with very diverse pharyngeal functions (Ragsdale et al. 2010; Zhang and Baldwin 2000). This evolutionary adaptability and robustness suggests that the nematode pharyngeal nervous system is highly degenerate, but this hypothesis has not been directly tested.

Testing for degeneracy and functional complexity requires identification of distinct neural elements or networks capable of producing identical outputs. In laser ablation experiments, neurons are killed in young larvae and behavior is observed in adult worms (Avery 1993a; Avery and Horvitz 1987, 1989; Raizen et al. 1995). This approach causes irreversible elimination of neuron function, is potentially confounded by redundancy and compensatory changes during development, and may fail to uncover effects on adult feeding behavior due to early larval lethality (Avery and Horvitz 1987). Optogenetic tools, which permit temporally precise manipulation of neural activity, can overcome limitations of laser ablation and directly identify roles of individual neurons in generating or regulating behavior (Zhang et al. 2007). Functional dissection of neural circuits using optogenetics requires either cell-specific opsin expression (Schmitt et al. 2012) or selective illumination of the neuron of interest after broad opsin expression (Guo et al. 2009; Kocabas et al. 2012; Leifer et al. 2011; Stirman et al. 2011).

To determine the roles of cholinergic pharyngeal neurons in pumping regulation and the pathways through which they act, we developed a technique for optogenetic manipulation of single neuron activity in vivo. Because pharyngeal behavior is completely internal to the animal, immobilizing the worms affords increased spatial resolution such that it is possible to manipulate individual pharyngeal neurons optogenetically and simultaneously record behavior. We confirm the endogenous excitatory role of the MCs and identify endogenous degenerate excitatory roles for the M2s, M4, and the I1s in a robust network that regulates feeding rate. We identify a state-dependent excitatory role for the I1s, and we illuminate degeneracy at the genetic level by identifying two molecular mechanisms that mediate the stimulatory role of the MCs.

MATERIALS AND METHODS

Worm strains. ZM3265 (*lin-15(n765ts) X; zxIs6[Punc-17::ChR2(H134R)::YFP; lin-15(+)] V*), ZX499 [*lin-15(n765ts) X; zxIs5[Punc-17::ChR2(H134R)::YFP; lin-15(+)] X*), and ZX830 (*lite-1(ce314) X; zxEx620[Punc-17::Mac::YFP; Pelt-2::mCherry*]) were gifts from A. Gottschalk (Husson et al. 2012; Liewald et al. 2008). After verification of expression in cholinergic pharyngeal neurons, we crossed ZM3265 into LX929 (*vsIs48[unc-17::GFP] X*), which has bright cytoplasmic green fluorescent protein (GFP) fluorescence in cholinergic neurons, to create YX11 (*lin-15(n765ts) X; zxIs6[Punc-17::ChR2(H134R)::YFP; lin-15(+)] V; vsIs48[unc-17::GFP] X*). We then crossed YX11 into DA1113 (*eat-2(ad1113) II*) (Avery 1993b),

DA1110 (*eat-18*(*ad1110*) *I*) (Raizen et al. 1995), and CB933 (*unc-17*(*e245*) *IV*) (Brenner 1974) to create YX46 (*eat-2(ad1113) II; vsIs48[unc-17::GFP] X; zxIs6[unc-17::ChR2(H134R)::YFP; lin-15(+)] V*), YX47 (*eat-18(ad1110) I; vsIs48[unc-17::GFP] X; zxIs6[unc-17::ChR2(H134R)::YFP; lin-15(+)]*), and YX48 (*unc-17(e245) IV; vsIs48[unc-17::GFP] X; zxIs6[unc-17::ChR2(H134R)::YFP; lin-15(+)]*), respectively. Since *gar-3* and *zxIs6* are both located on chromosome V, we had difficulty obtaining *gar-3; zxIs6* cross-progeny and adopted a different approach for experiments involving *gar-3*. We crossed VC657 (*gar-3(gk305) V*) (Liu et al. 2007) with DA1110 and with ZX499 to form YX66 (*eat-18(ad1110) I; gar-3(gk305) V*) and YX68 (*gar-3(gk305) V; zxIs5[unc-17::ChR2(H134R)::YFP; lin-15(+)] X*), respectively. We identified the presence of the *gk305* deletion mutation by PCR followed by agarose gel electrophoresis (primer sequences were 5′-TGTTCTGAGTTTTT-GCATTAAA-3′ and 5′-GGACATTTTCTGTATTTCTTTTTAC-3′). We crossed YX66 into YX68 to create YX69 (*eat-18(ad1110) I; gar-3(gk305) V; zxIs5[unc-17::ChR2(H134R)::YFP; lin-15(+)] X*). To rescue the *gar-3* defect, we used an Eppendorf FemtoJet microinjection system on a Leica DMIRB inverted differential interference contrast (DIC) microscope to inject the fosmid *WRM0627cH05* at 10 ng/μl in combination with 5 ng/μl pCFJ104*(myo-3::mCherry)*. We performed all experiments involving inhibition with ZX830. All optogenetics experiments were performed on first-day adult hermaphrodites.

We grew all worms in the dark at 20°C on NGM (Brenner 1974) plates inoculated with 250 μl of a suspension of OP50 bacteria in lysogeny broth (LB) medium. Where needed, we added 2 μl of 100 mM all-*trans*-retinal (ATR) in ethanol to the bacterial suspension immediately before seeding. We stored ATR-seeded plates at 4°C for up to 1 wk before use.

Laser ablations. We performed MC and M2 laser ablations as previously described (Bargmann and Avery 1995; Fang-Yen et al. 2012). Briefly, we immobilized L1 larvae in 15 mM sodium azide on 5% agarose pads within 4 h after hatching. With DIC optics on a Leica DM5500 B upright microscope equipped with a ×100 Plan Apo oil-immersion objective lens with 1.4 numerical aperture (NA), we identified and ablated neurons with 60–80 pulses from a Photonics Instruments MicroPoint laser. All ablations were confirmed via observation of DIC and/or fluorescence 2–3 days after the operation. All animals with collateral damage were discarded. Controls for laser ablation experiments were subject to the same immobilization protocols as operated animals, but the laser was not fired. We performed I1 ablations using equipment and methods as previously described (Avery and Horvitz 1987; Raizen et al. 1995).

Optogenetic stimulation of individual neurons. We mounted worms on 10% agarose pads containing 10 mM 5-HT and immobilized them using 1.5 μl of a 2.5% (vol/vol) suspension of 50-nm diameter polystyrene beads (Kim et al. 2013). We included 5 mM atropine in the agarose pad where indicated; we reduced the 5-HT concentration to 5 mM for these atropine experiments to compensate for the increased ionic concentration. This atropine concentration is half of that previously used to study the roles of muscarinic receptors in *C. elegans* feeding behavior (You et al. 2006). The *C. elegans* cuticle and intestinal lining generally limit drug uptake, and it is not unusual for polar drugs to be applied at concentrations 1,000-fold higher than their predicted target affinities (Holden-Dye and Walker 2007).

For each worm, we first illuminated the entire head with blue light for <1 s to image the fluorescent cholinergic neurons. Next, we subjected each relevant neuron type to a stimulus protocol consisting of 10 cycles of 5-s illumination and 5-s darkness. The stimulus area was determined by outlining a region slightly larger than the neural cell body, about 2–3 μm in diameter, to allow constant stimulation as the neural cell bodies move during the pump. *unc-17* Mutants did not immobilize well, likely due to their coiling behavior, so for these worms we used a larger spot of illumination, often covering the entire metacorpus. We performed experiments within 90 min of worm immobilization and performed each experiment on 7–10 animals unless otherwise indicated. This sample size was selected based on pilot data. For additional description of the approach, see RESULTS.

Microscopy and imaging. We used a setup similar to that described previously (Leifer et al. 2011; Fig. 1*E*). We performed optogenetic experiments on a Leica DMI3000 B microscope with a Leica Plan Apo ×63 oil-immersion objective lens with 1.4 NA. To stimulate individual neurons optogenetically, we expanded a 473-nm laser beam (Shanghai Laser & Optics Century) using a telescope composed of two plano-convex lenses and projected it onto a 1,024-by-768-pixel digital micromirror device (DMD; DLP Discovery 4100; Texas Instruments/Digital Light Innovations). We aligned the DMD such that when the DMD was in the on state, the reflected beam was aligned with the optical axis of the microscope objective after entering the microscope through a right-side auxiliary port. The light from the DMD was projected onto the back of the objective using an optical system composed of three lenses and a dichroic mirror. We mounted the dichroic mirror, which reflects 473-nm light while allowing transmission of wavelengths >500 nm, on a custom filter cube in the microscope filter turret. The irradiance of the laser at the objective was ~37 mW/mm^2, well above the saturation irradiance of channelrhodopsin-2 (ChR2; Grossman et al. 2011). To image behavior, we placed a red filter in the transillumination light path. We used an image splitter (Photometrics DV2) to record fluorescence and bright-field images simultaneously. We acquired images at a rate of 32.7 frames per second on a cooled CCD camera (Andor iXon 885). We analyzed the images using custom MATLAB scripts as well as the freely available package PIVlab, a time-resolved digital particle image velocimetry (PIV) tool for MATLAB.

Software and analysis. We used Andor Solis software to acquire images. We controlled the DMD using the Discovery 4100 software; DMD scripts were created in MATLAB using custom scripts. After data acquisition, we used MATLAB to identify times when the stimulation was switched between off and on states and to determine pumping rate and other parameters. MATLAB scripts are available on request. Student's *t*-test was used for all statistical comparisons unless otherwise noted, and each bar represents means ± SE. Sample sizes are given in the figure captions.

Measurement of ChR2 expression. ChR2 expression was approximated by calculating the average fluorescence pixel value of a region surrounding the cell body of each pharyngeal neuron that expressed *zxIs6[Punc-17::ChR2(H134R)::YFP; lin-15(+)]V*.

Measurements of pharyngeal pumping on an agar surface in the absence of food. We transferred well-fed I1-ablated adult animals, which had been grown on NGMSR plates (Avery 1993b) seeded with HB101 bacteria (rather than OP50, to minimize any effects of potential chronic starvation on behavior), to the unseeded agar surface of 5.5-cm diameter NGMSR plates. After 5 min of locomotion on the unseeded agar, we counted pumps for 1 min.

RESULTS

Optogenetic manipulation of specific pharyngeal neurons in intact, behaving animals. We used a DMD and laser with 473-nm wavelength to illuminate individual neurons (Guo et al. 2009; Leifer et al. 2011) in worms expressing specific opsins in all cholinergic neurons. To excite neurons, we used a yellow fluorescent protein (YFP)-tagged blue-light-sensitive ChR2 (Nagel et al. 2003, 2005). To inhibit neurons, we used a YFP-tagged blue-light-powered proton pump (Mac) from *Leptosphaeria maculans* (Chow et al. 2010; Husson et al. 2012; Waschuk et al. 2005). In some experiments, we coexpressed cytoplasmic GFP along with YFP-ChR2 to visualize the neurons more easily. We physically immobilized the animals against agarose pads using polystyrene nanoparticles (Kim et

al. 2013). This immobilization causes a cessation of pumping, so we added 10 mM 5-HT to the agarose pads to induce a submaximal basal pumping rate; a nonzero but submaximal pumping rate allowed us to measure inhibitory as well as excitatory effects. To locate each cholinergic pharyngeal neuron, we first acquired a full-field fluorescence image of the worm's head (Fig. 1*C*). We then specified a region for illumination based on the fluorescence image and used the DMD to illuminate the specified region (Fig. 1*D*). To image behavior and fluorescence simultaneously on the same camera while avoiding nonspecific opsin activation, we performed the experiments with a red glass filter in the transillumination light path (Fig. 1*E*). We imaged the worms through a DualView2 image splitter with red fluorescent protein (RFP) and GFP filters: the RFP channel captured DIC images, and the GFP channel captured fluorescence, which allowed us both to ensure proper targeting of each neuron and to correlate behavior with neuron stimulation.

Machine vision quantification of pharyngeal behavior during optogenetic stimulation. We used a PIV algorithm in MATLAB to track the velocity of a region of the anterior terminal bulb to quantify pumping rate (Fig. 1*B*). The velocity was found to be biphasic in shape (Fig. 1*F*). Each positive spike in velocity represented movement of the grinder toward the posterior, and each negative spike represented its return to the resting position. For each experiment, we set a velocity threshold, the crossing of which signified a single pump. This threshold was set to approximately half of the maximum velocity. We wrote MATLAB scripts to calculate the average pump rate during stimulus intervals (Fig. 1, *F* and *G*), which were determined post hoc by automated detection of changes in fluorescence occurring when a GFP- and/or YFP-expressing neuron is illuminated. Our system for automated detection of pharyngeal pumps was in excellent agreement with results from a manual counting of pumps based on slow-motion review of videos, with 99.3% sensitivity and 99.5% specificity.

The MC motor neurons are excitatory for pharyngeal pumping. The paired MC neurons have cell bodies in the metacorpus, have putative sensory endings in the pharyngeal lumen near the posterior end of the procorpus, and form synapses with pharyngeal muscles in the posterior metacorpus and anterior isthmus (Fig. 1, *A* and *C*; Albertson and Thomson 1976). Because laser ablation of the MC neurons in young larvae causes an 83% decrease in pump rate in adult animals (Raizen et al. 1995), we hypothesized that optogenetic stimulation of the MCs would increase pump rate. Indeed, we found that optogenetic excitation of the MC neurons stimulated pumping (Fig. 2*A*; Supplemental Video S1, available in the data supplement online at the *Journal of Neurophysiology* Web site). MC illumination did not excite pumping in the absence of the essential ChR2 cofactor ATR (Fig. 2*A*), indicating that the increased pump rate during MC illumination was due to activation of ChR2.

Processes of other cholinergic neurons pass close to the MC cell bodies (Fig. 1, *A* and *C*; Albertson and Thomson 1976), raising the possibility that the optogenetic illumination was stimulating pumping via nontargeted neurons. To test this possibility, we performed larval ablation of the MC neurons and tested whether stimulation of the region corresponding to the usual location of the MC cell bodies results in an increased pumping rate. We found no increase in pump rate (Fig. 2*A*), indicating that off-target effects of this optogenetic stimulation are negligible.

Serial section electron microscopic analysis of the pharyngeal nervous system has shown that the MC neurons make no chemical synapses onto other neurons and possess gap junction connections only with the paired M2 neurons (Albertson and Thomson 1976). To determine whether the behavioral effect of

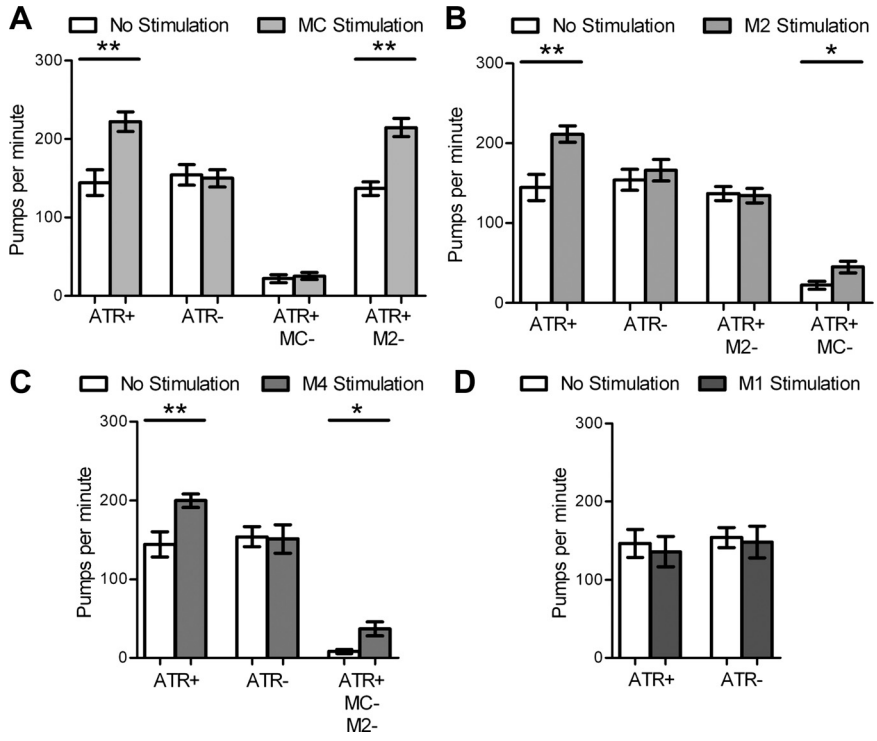

Fig. 2. Cholinergic motor neurons MC, M2, and M4, but not M1, are excitatory for pumping. *A*: MC stimulation excites pumping in an all-*trans*-retinal (ATR)-dependent manner. This effect is abolished when the MCs are ablated but not when the M2s are ablated. $n = 10, 7, 10, 9$ Animals for each pair of bars, respectively. *B*: M2 stimulation excites pumping in an ATR-dependent manner. This effect is abolished when the M2s are ablated but not when the MCs are ablated. $n = 10, 7, 10, 9$ Animals for each pair of bars, respectively. *C*: M4 stimulation excites pumping in an ATR-dependent manner. This effect persists when the MCs and the M2s are ablated. $n = 10, 7, 7$ Animals for each pair of bars, respectively. *D*: M1 stimulation does not excite pumping. $n = 9, 7$ Animals for each pair of bars, respectively. 5-HT (10 mM) was used for each experiment. Each bar represents mean ± SE. Statistical significance was calculated using the 2-tailed Student's *t*-test. $*P < 0.05$; $**P < 0.01$.

optogenetic stimulation of MC occurs wholly via effects on M2, we performed optogenetic excitation of the MCs in animals in which the M2 neurons were laser-ablated. Stimulation of the MCs still excited pumping after the ablation of the M2 neurons (Fig. 2*A*), demonstrating that the MCs can directly stimulate pumping.

The M2 motor neurons are excitatory for pharyngeal pumping. Anatomic data suggest that the paired M2 neurons make chemical synapses only onto pharyngeal muscles in the isthmus and metacorpus (Fig. 1, *A* and *C*; Albertson and Thomson 1976). However, ablation of the M2 neurons in young larvae results in only a 16% decrease in pump rate in adults (Raizen et al. 1995), suggesting a minor role for the M2s in pumping regulation. To our surprise, we found that optogenetic stimulation of the M2s increased pump rate to a similar level as that observed during MC stimulation (Fig. 2*B*; Supplemental Video S2). As with the MCs, this effect was ATR-dependent (Fig. 2*B*) and did not occur when the same region was stimulated after M2 ablation (Fig. 2*B*), demonstrating that specific activation of the M2s excites pumping. Furthermore, M2 excitation stimulated pumping in the absence of the MC neurons (Fig. 2*B*), demonstrating that the M2s, like the MCs, can stimulate pumping directly.

The M4 motor neuron is excitatory for pharyngeal pumping and isthmus peristalsis. The M4 neuron synapses only on the pharyngeal muscles in the isthmus and terminal bulb (Fig. 1, *A* and *C*; Albertson and Thomson 1976) and is the only neuron required for isthmus peristalsis (Avery and Horvitz 1987, 1989). Laser ablation experiments have shown a 28% reduction in pump rate in adult animals after M4 ablation in young larvae (Raizen et al. 1995). However, interpretation of this experiment is confounded by the peristalsis defect seen after M4 ablation: defective peristalsis causes both starvation, which itself causes a reduction in pump rate (Avery and Horvitz 1990), and distention of the corpus by bacteria, which may affect pharyngeal behavior via abnormal activation of mechanosensory endings (Avery and Horvitz 1987; Raizen et al. 1995). Our optogenetic approach allowed us to test directly whether M4 could stimulate pumping rate in well-fed animals with normal peristalsis. We found that optogenetic excitation of the M4 neuron caused an increase in pumping to a similar level as that observed during MC or M2 stimulation (Fig. 2*C*; Supplemental Video S3). No cholinergic pharyngeal neurons send processes behind the M4 cell body, so the effect of M4 stimulation is due to specific activation of M4. Consistent with its proposed role in regulating isthmus peristalsis, optogenetic excitation of M4 caused a greater proportion of pumps to be followed by peristalsis than during MC stimulation. During five 10-s intervals of M4 stimulation in two worms, 97% of pumps ($n = 179$ pumps) were followed by isthmus peristalsis, whereas during stimulation of MC in the same worms only 41% ($n = 204$ pumps) were followed by peristalsis ($P < 0.0002$, Mann-Whitney U test). M4 excitation caused an increase in pump rate in the absence of both the MCs and the M2s (Fig. 2*C*), demonstrating that M4 can directly stimulate pumping.

Stimulation of the M1 motor neuron does not excite pumping. The M1 neuron sends a process from the terminal bulb to the anterior end of the corpus, where it forms synapses on the anterior pharyngeal muscles (Fig. 1, *A* and *C*; Albertson and Thomson 1976). M1 ablation causes only an 8% reduction in pump rate (Raizen et al. 1995). In contrast to the other cholinergic pharyngeal neurons, we did not find M1 optogenetic stimulation to affect pump rate (Fig. 2*D*). This is unlikely to be explained by a lower level of expression of ChR2 in M1 since the average fluorescence intensity of *ChR2::YFP* in M1 was similar to that measured in MC, M2, and M4 (MC: 93.8 ± 7.1; M2: 101.2 ± 11.0; M4: 91.2 ± 10.7; M1: 71.6 ± 16.7; means ± SE, arbitrary units, $n = 6$; $P > 0.79$ 1-way ANOVA with Dunn's multiple-comparison test). These results suggest that M1 stimulation does not excite pharyngeal pumping.

The I1 interneurons have a state-dependent excitatory role in pumping regulation and can modulate pumping through the MCs and M2s. The paired I1 neurons form the only synaptic connections between the somatic and pharyngeal nervous systems and are the only cholinergic pharyngeal neurons that do not synapse onto pharyngeal muscle (Albertson and Thomson 1976). Ablation of the I1 neurons has no effect on the pump rate in the presence of food (Raizen et al. 1995). However, we found that the I1s are required for pumping in the absence of food (Fig. 3*A*). Electron microscopy data indicated that the I1s are presynaptic to six classes of neurons, including the MCs and the M2s but not M4 (Albertson and Thomson 1976). Optogenetic stimulation of the I1 neurons increases pumping rate in an ATR-dependent manner to a level similar to that seen with MC or M2 stimulation (Fig. 3*B*; Supplemental Video S4). No cholinergic pharyngeal neurons send processes behind the I1 cell body, so the effect of I1 stimulation is due to specific activation of I1. I1 stimulation excited pumping following the ablation of either the MCs or the M2s but not following

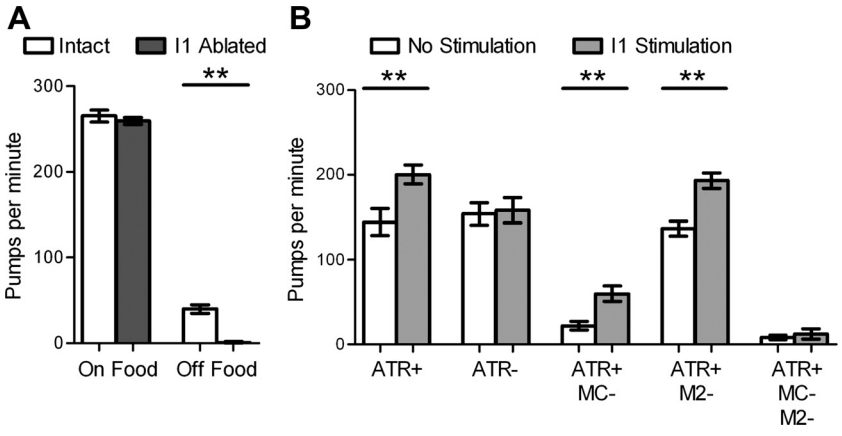

Fig. 3. The I1 interneurons are required for basal pumping and stimulate pumping via the MCs and the M2s. *A*: I1 ablation reduces pumping rate in the absence of food. $n = 8, 3, 46, 7$ Animals for each bar, respectively. See MATERIALS AND METHODS for details. *B*: I1 stimulates pumping in an ATR-dependent manner and in the absence of either the MCs or the M2s but not both. $n = 10, 7, 10, 9, 7$ Animals for each pair of bars, respectively. 5-HT (10 mM) was used for each experiment in *B*. Each bar represents mean ± SE. Statistical significance was calculated using the 2-tailed paired Student's *t*-test. $^{**}P < 0.01$.

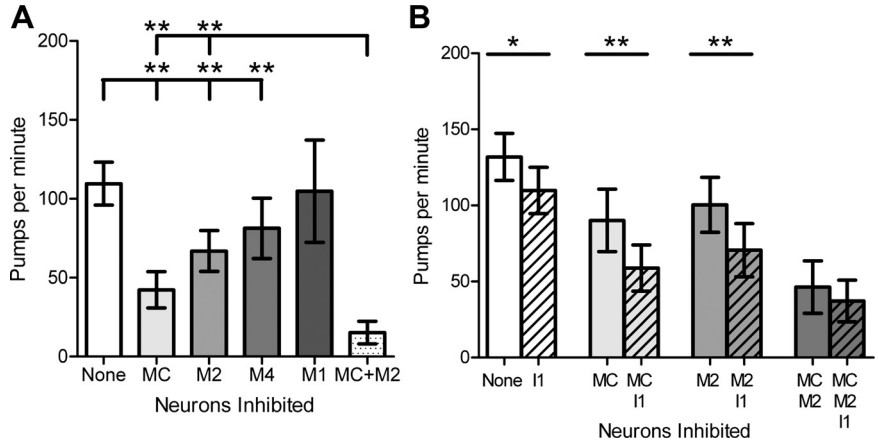

Fig. 4. Optogenetic inhibition of pharyngeal cholinergic neurons inhibits 5-HT-stimulated pumping. *A*: optogenetic inhibition of the MCs, the M2s, and M4, but not M1, inhibits 5-HT-stimulated pumping. Simultaneous inhibition of the MCs and the M2s causes an inhibition of pumping greater than that observed during inhibition of either the MCs or the M2s alone, consistent with an endogenous role for the M2s in pumping regulation. "None" indicates that no neurons were inhibited. $n = 15$ For control, 14 for the MCs, 13 for the M2s, 9 for M4, and 4 for M1. *B*: inhibition of the I1s inhibits 5-HT-stimulated pumping. Simultaneous I1 inhibition increased the effects of individual MC inhibition or M2 inhibition, but not of combined MC and M2 inhibition, indicating that I1 stimulates pumping endogenously via the MCs and the M2s. $n = 9$ For each bar. 5-HT (10 mM) was used for each experiment. Each bar represents mean ± SE. Statistical significance was calculated using the 2-tailed Student's *t*-test. $*P < 0.05$; $**P < 0.01$.

ablation of both neuron types (Fig. 3*B*), demonstrating that the I1s can stimulate pumping through the MCs, through the M2s, or through both the MCs and the M2s.

The MC, M2, and M4 motor neurons stimulate pumping endogenously. Our optogenetic experiments with ChR2 showed that the MC, M2, M4, and I1 neurons are capable of stimulating pumping. However, it does not necessarily follow that these neurons endogenously regulate pumping rate. To determine whether these neurons stimulate pumping endogenously, we expressed the proton pump Mac in the cholinergic neurons (Husson et al. 2012) and individually inhibited these neurons using methods otherwise identical to those used with ChR2. We found that optogenetic inhibition of the MCs, the M2s, or M4 reduced pump rate, indicating that an endogenous function of these neurons is to stimulate pumping (Fig. 4*A*). By contrast, optogenetic inhibition of M1 had no effect on pump rate, suggesting that M1 is not required for pump rate regulation. Simultaneous inhibition of the MCs and the M2s caused a greater inhibition of pumping than inhibition of either alone, consistent with an endogenous role for the M2s in pumping rate regulation (Fig. 4*A*).

The I1 interneurons regulate pumping endogenously via the MCs and the M2s. As with MC, M2, and M4, we found that I1 inhibition caused a decrease in pumping (Fig. 4*B*). To test whether the I1s endogenously act through the MCs and the M2s to regulate pump rate, as our ChR2 experiments suggested, we simultaneously inhibited the I1s and the MCs, the M2s, or both the MCs and the M2s. Inhibition of the I1s simultaneously with inhibition of the MCs caused a stronger reduction in pump rate than inhibition of the MCs alone, suggesting that the I1s can function independently of the MCs. Similarly, inhibition of the I1s simultaneously with inhibition of the M2s caused a stronger pump rate reduction than inhibition of the M2s alone, suggesting that the I1s can function independently of the M2s. However, inhibition of the I1s simultaneously with inhibition of both the MCs and the M2s did not cause slower pumping than that seen with inhibition of the MCs and the M2s alone (Fig. 4*B*), indicating that effect of I1 inhibition on pumping rate requires the MCs and the M2s. Together with our ChR2 stimulation data, these results indicate that the I1s endogenously excite pumping via both the MCs and the M2s.

The MC neurons can stimulate pumping through a nonnicotinic mechanism. Mutations in the gene *eat-2*, which encodes a nicotinic ACh receptor subunit expressed in pharyngeal muscle postsynaptic to the MCs (McKay et al. 2004), causes a reduced pump rate that mimics the phenotype observed after MC ablation (Avery 1993b; Raizen et al. 1995). This observation suggested that the mechanism by which the MC neurons stimulate feeding is via activation of a nicotinic ACh receptor containing EAT-2. Therefore, we expected that stimulation of the MCs in *eat-2* mutants would not increase pump rate. To our surprise, we found that stimulation of the MC neurons in *eat-2* mutants causes an increase in pumping, albeit less than in wild-type worms (Fig. 5 vs. Fig. 2*A*). Stimulation of the same region following MC ablation in wild-type worms did not cause an increase in pumping (Fig. 2*A*), demonstrating that this effect is not due to off-target excitation of nearby processes. These results demonstrate that the MCs can stimulate pumping through an EAT-2-independent mechanism.

To test the possibility that the MCs can stimulate pumping via an alternative nicotinic ACh receptor in the absence of EAT-2, we studied animals lacking EAT-18, a single transmembrane protein required for the pharyngeal response to bath-applied nicotine (McKay et al. 2004; Raizen et al. 1995). In *eat-18* mutants, the staining of the pharynx with α-bungarotoxin, which binds to nicotinic ACh receptors, is also eliminated (McKay et al. 2004). As in the absence of EAT-2, optogenetic stimulation of the MCs resulted in a pumping increase in the absence of EAT-18 (Fig. 5), suggesting that the MCs can excite pumping via a nonnicotinic mechanism.

The MC neurons directly stimulate pumping via a nonnicotinic cholinergic mechanism. To explore further the nature of the EAT-2- and EAT-18-independent MC-induced pumping, we examined mutants for the gene *unc-17*, which encodes a transporter required for loading ACh into vesicles before release (Alfonso et al. 1993). Since *unc-17* null mutations are lethal, we used the hypomorphic allele *e245*, which had a

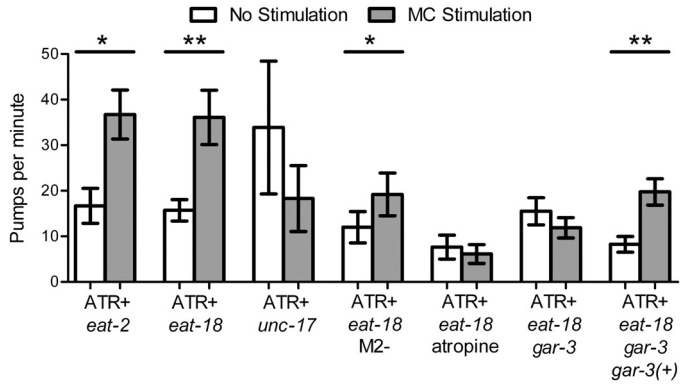

Fig. 5. The MCs can directly excite pumping via both nicotinic and muscarinic receptors. Optogenetic MC stimulation increases pumping in both *eat-2* and *eat-18* nicotinic receptor mutants but not in *unc-17* (vesicular ACh transporter) mutants, demonstrating that MC can act via a nonnicotinic cholinergic pathway in addition to the known EAT-2/EAT-18 nicotinic pathway. Serial section electron microscopy suggests that the MCs and M2s form gap junctions; MC stimulation directly increases pumping in the absence of the M2s in *eat-18* mutants. MC stimulation does not increase pumping in *eat-18* mutants in the presence of the muscarinic antagonist atropine. GAR-3 is a muscarinic receptor expressed in pharyngeal muscle; MC stimulation does not increase pumping in *eat-18; gar-3* double mutants. Injection of a transgene containing the *gar-3* genomic region restores the ability of MC stimulation to excite pumping in *eat-18*; *gar-3* mutants. n = 10, 10, 8, 9, 9, 10, 10 Animals for each pair of bars, respectively. 5-HT (10 mM) was used for each experiment except those with atropine, where we used 5 mM 5-HT and 5 mM atropine. Each bar represents mean ± SE. Statistical significance was calculated using the 2-tailed Student's t-test. $^*P < 0.05$; $^{**}P < 0.01$.

variable basal pumping rate during immobilization. Stimulation of the pharyngeal metacorpus, which includes the MC cell bodies and processes, did not increase pumping rate in *unc-17* mutants (Fig. 5), demonstrating that MC stimulation of pumping requires cholinergic neurotransmission.

The MCs may stimulate pumping via a cholinergic nonnicotinic mechanism by acting directly on pharyngeal muscle, or they may act via their electrical connections to the M2s. To distinguish between these possibilities, we tested the effect of MC stimulation in *eat-18* mutants in which we ablated the M2 neurons. MC stimulation still increased pumping in *eat-18* mutants in the absence of the M2s (Fig. 5), demonstrating that the MCs can activate pumping directly via a cholinergic nonnicotinic mechanism.

The MC neurons stimulate pumping in part via the muscarinic receptor GAR-3. Ionotropic cholinergic receptors insensitive to nicotine have been identified in *C. elegans* (Francis et al. 2005; Richmond and Jorgensen 1999; Touroutine et al. 2005), suggesting the possibility that MC stimulates pumping in an *eat-18* genetic background through such a channel. Alternatively, the MCs may be acting through a muscarinic receptor. To distinguish between these possibilities, we used the muscarinic antagonist atropine (You et al. 2006). In the presence of atropine, MC stimulation failed to excite pumping in *eat-18* mutants (Fig. 5), demonstrating that in the absence of *eat-18*, the MCs stimulate pumping via an atropine-sensitive receptor and hence likely a muscarinic ACh receptor.

The *C. elegans* genome contains three genes that encode for muscarinic receptors: *gar-1* (Lee et al. 1999), *gar-2* (Lee et al. 2000), and *gar-3* (Hwang et al. 1999). Of these, only *gar-3* has been reported to be expressed in pharyngeal muscle (Steger and Avery 2004). Loss of GAR-3 has been shown to cause decreased action potential duration in pharyngeal muscle, and excessive GAR-3 signaling can cause muscle contraction to outlast muscle depolarization (Steger and Avery 2004), consistent with an excitatory role for GAR-3 in response to MC stimulation. We therefore tested whether the MCs excite pumping via GAR-3 in an *eat-18* mutant background. MC stimulation did not excite pumping in *eat-18; gar-3* double mutants (Fig. 5), demonstrating that the MCs activate pumping in part through the muscarinic ACh receptor GAR-3. A transgene containing the *gar-3* gene restored the ability of MC stimulation to excite pumping in *eat-18; gar-3* double mutants (Fig. 5), confirming that the *gar-3* mutation caused the defect in the ability of the MCs to excite pumping in the absence of EAT-18.

DISCUSSION

By optogenetically manipulating individual *C. elegans* neurons while recording feeding behavior, we have shown that the cholinergic MC, M2, and M4 motor neurons stimulate pharyngeal pumping in a degenerate manner (Fig. 6). The cholinergic I1 interneurons stimulate pumping via the MCs and the M2s and act in a state-dependent manner to stimulate pumping in the absence of food. By analysis of mutants, we identified nicotinic and muscarinic pathways through which the MCs regulate pumping rate. Taken together, these results demonstrate that this robust and evolutionarily adaptable network is highly degenerate at both the neural and genetic levels and that the same behavior can be stimulated by multiple neurons and through different types of receptors.

An optogenetic approach reveals novel functions for multiple neurons. Although optogenetic tools have played an important role in clarifying the functional dynamics of identified neural networks, to our knowledge they have not been previously used to identify new functional roles of circuit elements in *C. elegans* (Husson et al. 2013). In contrast to laser ablation, single neuron optogenetic manipulation allows us to test the roles of individual neurons in regulating behavior while avoiding the possibilities of developmental compensation and ablation-induced developmental abnormalities, phenomena that would be expected to occur in degenerate networks (Marder and Taylor 2011). For example, M4 ablation results in early larval lethality (Avery and Horvitz 1987), which prevents accurate assessment of its effects on feeding rates in adult animals. In *eat-2* mutants, the resting membrane potential of the terminal bulb is depolarized and unstable relative to wild-type worms (Steger et al. 2005). It is possible that similar

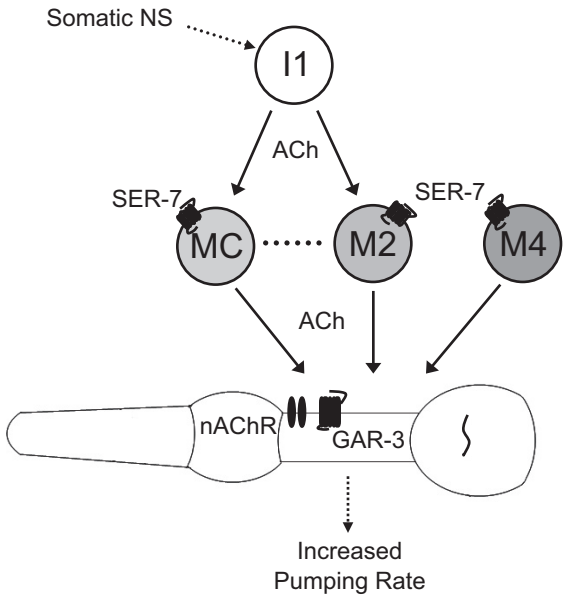

Fig. 6. Model of the cholinergic network regulating feeding rate. The MCs, the M2s, and M4 can directly stimulate pumping, and the I1s can stimulate pumping via the MCs and the M2s. The MCs and the M2s are connected by gap junctions. The serotonin receptor SER-7 is expressed in the MCs, the M2s, and M4. The MCs stimulate pumping via a nicotinic receptor containing EAT-2 and EAT-18 and also via the GAR-3 muscarinic receptor. NS, nervous system; nAChR, nicotinic ACh receptor.

compensation occurs after ablation of pharyngeal neurons, either in the muscle or other neurons.

The candidate neuron and gene approach we demonstrate here is especially well-suited for identifying components of degenerate networks, in which ablation of individual classes of neurons may not cause obvious phenotypes. For example, although laser ablation of the M2s yields only a small reduction in pumping rate (Raizen et al. 1995), we found that M2 excitation stimulates rapid pumping. It is possible that other excitatory cholinergic neurons, such as the MCs and M4, replace this function of the M2s after their ablation. Likewise, whereas *gar-3* mutants have only subtle feeding defects (Steger and Avery 2004), we found that the MCs can act via GAR-3 to stimulate pumping in the absence of EAT-18. Indeed, one characteristic of degenerate neural networks is that specific faults in the system, such as focused neurological lesions, often do not cause changes in outputs (Gazzaniga 1995).

Our approach is also well-suited for identifying the molecular mechanisms through which individual neurons can stimulate pumping. We have identified two distinct cholinergic receptors postsynaptic to the MCs, and we expect that receptors downstream of other neurons could be identified by a similar approach of testing whether optogenetic stimulation of individual neurons can still stimulate pumping in mutants for candidate genes. For example, testing the effects of mutations in different nicotinic ACh receptor subunits expressed in pharyngeal muscle on the excitatory effects of stimulating the M2s or M4 should lead to the identification of the receptors postsynaptic to these neurons.

Another advantage of our approach is its ability to assess individually the function of multiple classes of neurons in the same animal. Studies in the crustacean stomatogastric ganglion have observed significant animal-to-animal variability in the tuning of neuron conductance parameters despite similar network output (Marder 2011; Prinz et al. 2004). Therefore, sequentially and nondestructively manipulating the activity of individual or multiple neurons in a single animal can provide a more complete picture of network function than one based on more sparse measurements in multiple animals.

Degeneracy at two levels allows robust responses to unpredictable environmental and physiological signals. Our work has revealed that a circuit that tightly regulates response to various intrinsic and extrinsic cues has degeneracy at both the neural and genetic levels. Feeding rate in *C. elegans* is influenced by a multitude of factors, including mechanosensation (Chalfie et al. 1985), chemosensation (Li et al. 2012), heat stress (Jones and Candido 1999), aging (Huang et al. 2004), mating (Gruninger et al. 2006), starvation (Avery and Horvitz 1990), food quality (Soukas et al. 2009), feeding history (Song et al. 2013), satiety (You et al. 2008), molting (Cassada and Russell 1975), sleep (Raizen et al. 2008), and infection (Los et al. 2013). Degeneracy at multiple levels allows the pharyngeal nervous system to integrate these inputs to determine feeding rate (Cunningham et al. 2012; Greer et al. 2008; Li et al. 2012). The neural degeneracy of the system allows multiple neurons to perform similar functions in response to different modulators, whereas the genetic degeneracy allows neurotransmitters and neuropeptides to activate subsets of neurons or muscles differentially or to activate different cell signaling cascades within the same neuron or muscle. Having improved our definition of the circuit that regulates feeding rate, we are now in a better position to understand the circuit mechanisms by which intrinsic and extrinsic cues affect behavior.

Depolarization and 5-HT stimulation of the same pharyngeal neuron can cause similar or distinct behaviors. 5-HT is a potent modulator of many *C. elegans* behaviors, including feeding (Chase and Koelle 2007). We found that basal pumping is almost completely abolished in immobilized worms in the absence of 5-HT, but MC, M2, M4, or I1 stimulation caused a small but variable increase in pump rate (data not shown). This is likely because when the worm is immobilized, the stimulus-response curve of the neurons is not linear, so that even a large stimulus causes only a small neural response.

The 5-HT G protein-coupled receptor SER-7 is expressed in many pharyngeal neurons, including the MCs, the M2s, and M4 (Fig. 6; Hobson et al. 2005). 5-HT stimulates pumping primarily by activating SER-7 in the MCs (Song and Avery 2012). We suspect that the basal pumping rate we observe in the presence of 5-HT is also due to activation of SER-7 in the MCs, since MC ablation dramatically decreases the pump rate on 5-HT in our experiments (Fig. 2*A*). Interestingly, whereas activation of SER-7 in M4 causes increased peristalsis but not pumping (Song and Avery 2012), we found that optogenetic stimulation of M4 causes an increase in both pumping and peristalsis rates. It is likely that depolarization and SER-7 activation stimulate intracellular pathways that are at least partially distinct, which in turn evokes neurotransmitter release that may differ in location, amount, or molecular identity.

Functional conservation and evolutionary adaptability of the pharyngeal nervous system. It has been postulated that the processes of evolution and natural selection necessarily are accompanied by degeneracy (Edelman and Gally 2001), but this is a challenging idea to test experimentally. The prevalence of evolutionarily divergent nematode species and the relative ease with which their pharyngeal nervous systems can be

anatomically mapped makes them interesting models for studying the role of degeneracy in evolution. However, despite the apparent simplicity of the anatomic connectivity of the pharynx, inferring the function of the pharyngeal nervous system from the wiring diagram alone is difficult. The sign of physiological connections is often unknown, and the number of synapses between two cells does not always correlate with the importance of this connection (Bargmann and Marder 2013; Chalfie et al. 1985). For example, although the M2s form 60 synapses on pharyngeal muscle and the MCs form just 4 (Albertson and Thomson 1976; Avery and Thomas 1997; Avery and You 2012; McKay et al. 2004), we find that effects of stimulation of these 2 neuron types on pumping rate are equivalent (Fig. 2, *A* and *B*). Thus, without knowledge of the functional connectivity, it is difficult to interpret the differences between the wiring of *C. elegans* and other species, such as *P. pacificus*, in an evolutionary context (Bumbarger et al. 2013).

Laser ablation data from other nematode species may be informative. Ablation of M4 causes a reduction in isthmus peristalsis in every species in which it has been tested, including *P. pacificus*, demonstrating a conserved function (Chiang et al. 2006). The M2s synapse on the anterior pharyngeal muscle in *C. elegans* and *P. pacificus*, and ablation of the M2s in *Panagrolaimus* sp. PS1159 causes a decrease in anterior isthmus peristalsis, a behavior observed in neither *C. elegans* nor *P. pacificus* (Chiang et al. 2006). Ablation of either the MCs or M4 in *P. pacificus* and either the M2s or M4 in *Panagrolaimus* sp. PS1159 causes a decrease in pumping rate (Chiang et al. 2006), demonstrating that the networks regulating feeding are also degenerate in these species. Although further experiments are necessary to draw firm conclusions, these data are consistent with evolutionary adaptability, functional conservation, and degeneracy of pharyngeal nervous system function in different species.

A circuit-level framework for feeding modulation. By identifying the pathways of cholinergic input that regulate pharyngeal pumping rate (Fig. 6), this work defines a framework within which we can investigate how feeding is integrated with other physiological processes and behaviors in response to changing environmental and internal states. The method described here can be used to develop further this circuit-level framework by identifying roles for the remaining nine classes of pharyngeal neurons as well as the molecular mechanisms through which they interact. This method also can be combined with genetically encoded calcium indicators to visualize intracellular calcium dynamics during optogenetic manipulation (Husson et al. 2013). The functional connectivity of the pharyngeal circuit forms a foundation for exploring how mutations affect the activity of a degenerate network and how the network adapts to regulate behavior robustly.

ACKNOWLEDGMENTS

We thank Alexander Gottschalk for sharing strains ZM3265, ZX499, and ZX830.

GRANTS

Some strains were provided by the *Caenorhabditis* Genetics Center (CGC), which is funded by National Institutes of Health (NIH) Office of Research Infrastructure Programs (P40-OD-010440). This work was supported by the National Institute of Neurological Disorders and Stroke of the NIH under Awards R01-NS-064030 (D. M. Raizen) and R01-NS-084835 (C. Fang-Yen), the National Heart, Lung, and Blood Institute of the NIH Award T31-HL-07953 (N. F. Trojanowski; principal investigator: Allen I. Pack), a Brain & Behavior Research Foundation [formerly National Alliance for Research on Schizophrenia and Depression (NARSAD)] Young Investigator Award (D. M. Raizen), the Ellison Medical Foundation (C. Fang-Yen), and an Alfred P. Sloan Foundation Research Fellowship (C. Fang-Yen).

DISCLOSURES

No conflicts of interest, financial or otherwise, are declared by the author(s).

AUTHOR CONTRIBUTIONS

N.F.T., O.P.-M., D.M.R., and C.F.-Y. conception and design of research; N.F.T. and D.M.R. performed experiments; N.F.T., D.M.R., and C.F.-Y. analyzed data; N.F.T., D.M.R., and C.F.-Y. interpreted results of experiments; N.F.T. and O.P.-M. prepared figures; N.F.T. drafted manuscript; N.F.T., O.P.-M., D.M.R., and C.F.-Y. edited and revised manuscript; N.F.T., O.P.-M., D.M.R., and C.F.-Y. approved final version of manuscript.

REFERENCES

Albertson DG, Thomson JN. The pharynx of *Caenorhabditis elegans*. *Philos Trans R Soc Lond B Biol Sci* 275: 299–325, 1976.

Alfonso A, Grundahl KM, Duerr JS, Han HP, Rand JB. The *Caenorhabditis elegans* unc-17 gene: a putative vesicular acetylcholine transporter. *Science* 261: 617–619, 1993.

Avery L. Motor neuron M3 controls pharyngeal muscle relaxation timing in *Caenorhabditis elegans*. *J Exp Biol* 175: 283–297, 1993a.

Avery L. The genetics of feeding in *Caenorhabditis elegans*. *Genetics* 133: 897–917, 1993b.

Avery L, Horvitz HR. A cell that dies during wild-type *C. elegans* development can function as a neuron in a ced-3 mutant. *Cell* 51: 1071–1078, 1987.

Avery L, Horvitz HR. Effects of starvation and neuroactive drugs on feeding in *Caenorhabditis elegans*. *J Exp Zool* 253: 263–270, 1990.

Avery L, Horvitz HR. Pharyngeal pumping continues after laser killing of the pharyngeal nervous system of *C. elegans*. *Neuron* 3: 473–485, 1989.

Avery L, Thomas JH. Feeding and defecation: section II. Feeding. In: *C. elegans II* (2nd ed.). Cold Spring Harbor, NY: Cold Spring Harbor Laboratory Press, 1997, vol. 33, p. 679–716.

Avery L, You YJ. *C. elegans* feeding. *WormBook*. First published May 21, 2012; doi:10.1895/wormbook.1.150.1.

Bargmann CI, Avery L. Laser killing of cells in *Caenorhabditis elegans*. *Methods Cell Biol* 48: 225–250, 1995.

Bargmann CI, Marder E. From the connectome to brain function. *Nat Methods* 10: 483–490, 2013.

Brenner S. The genetics of *Caenorhabditis elegans*. *Genetics* 77: 71–94, 1974.

Bumbarger DJ, Riebesell M, Rödelsperger C, Sommer RJ. System-wide rewiring underlies behavioral differences in predatory and bacterial-feeding nematodes. *Cell* 152: 109–119, 2013.

Cassada RC, Russell RL. The dauerlarva, a post-embryonic developmental variant of the nematode *Caenorhabditis elegans*. *Dev Biol* 46: 326–342, 1975.

Chalfie M, Sulston JE, White JG, Southgate E, Thomson JN, Brenner S. The neural circuit for touch sensitivity in *Caenorhabditis elegans*. *J Neurosci* 5: 956–964, 1985.

Chase DL, Koelle MR. Biogenic amine neurotransmitters in *C. elegans*. *WormBook*. First published February 20, 2007; doi:10.1895/wormbook.1.132.1.

Chiang JT, Steciuk M, Shtonda BB, Avery L. Evolution of pharyngeal behaviors and neuronal functions in free-living soil nematodes. *J Exp Biol* 209: 1859–1873, 2006.

Chow BY, Han X, Dobry AS, Qian X, Chuong AS, Li M, Henninger MA, Belfort GM, Lin Y, Monahan PE, Boyden ES. High-performance genetically targetable optical neural silencing by light-driven proton pumps. *Nature* 463: 98–102, 2010.

Cunningham KA, Hua Z, Srinivasan S, Liu J, Lee BH, Edwards RH, Ashrafi K. AMP-activated kinase links serotonergic signaling to glutamate release for regulation of feeding behavior in *C. elegans*. *Cell Metab* 16: 113–121, 2012.

Dieterich C, Clifton SW, Schuster LN, Chinwalla A, Delehaunty K, Dinkelacker I, Fulton L, Fulton R, Godfrey J, Minx P, Mitreva M, Roeseler W, Tian H, Witte H, Yang SP, Wilson RK, Sommer RJ. The

Pristionchus pacificus genome provides a unique perspective on nematode lifestyle and parasitism. *Nat Genet* 40: 1193–1198, 2008.

Doncaster CC. Nematode feeding mechanisms. 1. Observations on *Rhabditis* and *Pelodera*. *Nematologica* 8: 313–320, 1962.

Edelman GM, Gally JA. Degeneracy and complexity in biological systems. *Proc Natl Acad Sci USA* 98: 13763–13768, 2001.

Fang-Yen C, Gabel CV, Samuel AD, Bargmann CI, Avery L. Laser microsurgery in *Caenorhabditis elegans*. *Methods Cell Biol* 107: 177–206, 2012.

Francis MM, Evans SP, Jensen M, Madsen DM, Mancuso J, Norman KR, Maricq AV. The Ror receptor tyrosine kinase CAM-1 is required for ACR-16-mediated synaptic transmission at the *C. elegans* neuromuscular junction. *Neuron* 46: 581–594, 2005.

Gazzaniga MS. Principles of human brain organization derived from split-brain studies. *Neuron* 14: 217–228, 1995.

Grashow R, Brookings T, Marder E. Compensation for variable intrinsic neuronal excitability by circuit-synaptic interactions. *J Neurosci* 30: 9145–9156, 2010.

Greer ER, Pérez CL, Van Gilst MR, Lee BH, Ashrafi K. Neural and molecular dissection of a *C. elegans* sensory circuit that regulates fat and feeding. *Cell Metab* 8: 118–131, 2008.

Grossman N, Nikolic K, Toumazou C, Degenaar P. Modeling study of the light stimulation of a neuron cell with channelrhodopsin-2 mutants. *IEEE Trans Biomed Eng* 58: 1742–1751, 2011.

Gruninger TR, Gualberto DG, LeBoeuf B, Garcia LR. Integration of male mating and feeding behaviors in *Caenorhabditis elegans*. *J Neurosci* 26: 169–179, 2006.

Guo ZV, Hart AC, Ramanathan S. Optical interrogation of neural circuits in *Caenorhabditis elegans*. *Nat Methods* 6: 891–896, 2009.

Gutierrez GJ, O'Leary T, Marder E. Multiple mechanisms switch an electrically coupled, synaptically inhibited neuron between competing rhythmic oscillators. *Neuron* 77: 845–858, 2013.

Hobson RJ, Hapiak VM, Xiao H, Buehrer KL, Komuniecki PR, Komuniecki RW. SER-7, a *Caenorhabditis elegans* 5-HT7-like receptor, is essential for the 5-HT stimulation of pharyngeal pumping and egg laying. *Genetics* 172: 159–169, 2005.

Holden-Dye L, Walker RJ. Anthelmintic drugs. *WormBook*. First published November 2, 2007; doi:10.1895/wormbook.1.143.1.

Huang C, Xiong C, Kornfeld K. Measurements of age-related changes of physiological processes that predict lifespan of *Caenorhabditis elegans*. *Proc Natl Acad Sci USA* 101: 8084–8089, 2004.

Husson SJ, Gottschalk A, Leifer AM. Optogenetic manipulation of neural activity in *C. elegans*: from synapse to circuits and behaviour. *Biol Cell* 105: 235–250, 2013.

Husson SJ, Liewald JF, Schultheis C, Stirman JN, Lu H, Gottschalk A. Microbial light-activatable proton pumps as neuronal inhibitors to functionally dissect neuronal networks in *C. elegans*. *PLoS One* 7: e40937, 2012.

Hwang JM, Chang DJ, Kim US, Lee YS, Park YS, Kaang BK, Cho NJ. Cloning and functional characterization of a *Caenorhabditis elegans* muscarinic acetylcholine receptor. *Receptors Channels* 6: 415–424, 1999.

Jones D, Candido EP. Feeding is inhibited by sublethal concentrations of toxicants and by heat stress in the nematode *Caenorhabditis elegans*: relationship to the cellular stress response. *J Exp Zool* 284: 147–157, 1999.

Kim E, Sun L, Gabel CV, Fang-Yen C. Long-term imaging of *Caenorhabditis elegans* using nanoparticle-mediated immobilization. *PLoS One* 8: e53419, 2013.

Kocabas A, Shen CH, Guo ZV, Ramanathan S. Controlling interneuron activity in *Caenorhabditis elegans* to evoke chemotactic behaviour. *Nature* 490: 273–277, 2012.

Lee YS, Park YS, Chang DJ, Hwang JM, Min CK, Kaang BK, Cho NJ. Cloning and expression of a G protein-linked acetylcholine receptor from *Caenorhabditis elegans*. *J Neurochem* 72: 58–65, 1999.

Lee YS, Park YS, Nam S, Suh S, Lee J, Kaang BK, Cho NJ. Characterization of GAR-2, a novel G protein-linked acetylcholine receptor from *Caenorhabditis elegans*. *J Neurochem* 75: 1800–1809, 2000.

Leifer AM, Fang-Yen C, Gershow M, Alkema MJ, Samuel AD. Optogenetic manipulation of neural activity in freely moving *Caenorhabditis elegans*. *Nat Methods* 8: 147–152, 2011.

Li Z, Li Y, Yi Y, Huang W, Yang S, Niu W, Zhang L, Xu Z, Qu A, Wu ZX, Xu T. Dissecting a central flip-flop circuit that integrates contradictory sensory cues in *C. elegans* feeding regulation. *Nat Commun* 3: 776, 2012.

Liewald JF, Brauner M, Stephens GJ, Bouhours M, Schultheis C, Zhen M, Gottschalk A. Optogenetic analysis of synaptic function. *Nat Methods* 5: 895–902, 2008.

Liu Y, LeBoeuf B, Garcia LR. Gα_q-coupled muscarinic acetylcholine receptors enhance nicotinic acetylcholine receptor signaling in *Caenorhabditis elegans* mating behavior. *J Neurosci* 27: 1411–1421, 2007.

Los FC, Ha C, Aroian RV. Neuronal Goα and CAPS regulate behavioral and immune responses to bacterial pore-forming toxins. *PLoS One* 8: e54528, 2013.

Marder E. Variability, compensation, and modulation in neurons and circuits. *Proc Natl Acad Sci USA* 108, *Suppl* 3: 15542–15548, 2011.

Marder E, Taylor AL. Multiple models to capture the variability in biological neurons and networks. *Nat Neurosci* 14: 133–138, 2011.

McKay JP, Raizen DM, Gottschalk A, Schafer WR, Avery L. *eat-2* and *eat-18* are required for nicotinic neurotransmission in the *Caenorhabditis elegans* pharynx. *Genetics* 166: 161–169, 2004.

Nagel G, Brauner M, Liewald JF, Adeishvili N, Bamberg E, Gottschalk A. Light activation of channelrhodopsin-2 in excitable cells of *Caenorhabditis elegans* triggers rapid behavioral responses. *Curr Biol* 15: 2279–2284, 2005.

Nagel G, Szellas T, Huhn W, Kateriya S, Adeishvili N, Berthold P, Ollig D, Hegemann P, Bamberg E. Channelrhodopsin-2, a directly light-gated cation-selective membrane channel. *Proc Natl Acad Sci USA* 100: 13940–13945, 2003.

Pires-daSilva A, Sommer RJ. Conservation of the global sex determination gene tra-1 in distantly related nematodes. *Genes Dev* 18: 1198–1208, 2004.

Prinz AA, Bucher D, Marder E. Similar network activity from disparate circuit parameters. *Nat Neurosci* 7: 1345–1352, 2004.

Ragsdale EJ, Ngo PT, Crum J, Ellisman MH, Baldwin JG. Reconstruction of the pharyngeal corpus of *Aphelenchus avenae* (Nematoda: Tylenchomorpha), with implications for phylogenetic congruence. *Zool J Linn Soc* 161: 1–30, 2010.

Raizen DM, Lee RY, Avery L. Interacting genes required for pharyngeal excitation by motor neuron MC in *Caenorhabditis elegans*. *Genetics* 141: 1365–1382, 1995.

Raizen DM, Zimmerman JE, Maycock MH, Ta UD, You YJ, Sundaram MV, Pack AI. Lethargus is a *Caenorhabditis elegans* sleep-like state. *Nature* 451: 569–572, 2008.

Richmond JE, Jorgensen EM. One GABA and two acetylcholine receptors function at the *C. elegans* neuromuscular junction. *Nat Neurosci* 2: 791–797, 1999.

Rodriguez JC, Blitz DM, Nusbaum MP. Convergent rhythm generation from divergent cellular mechanisms. *J Neurosci* 33: 18047–18064, 2013.

Saideman SR, Blitz DM, Nusbaum MP. Convergent motor patterns from divergent circuits. *J Neurosci* 27: 6664–6674, 2007.

Schmitt C, Schultheis C, Husson SJ, Liewald JF, Gottschalk A. Specific expression of channelrhodopsin-2 in single neurons of *Caenorhabditis elegans*. *PLoS One* 7: e43164, 2012.

Song BM, Avery L. Serotonin activates overall feeding by activating two separate neural pathways in *Caenorhabditis elegans*. *J Neurosci* 32: 1920–1931, 2012.

Song BM, Faumont S, Lockery SR, Avery L. Recognition of familiar food activates feeding via an endocrine serotonin signal in *Caenorhabditis elegans*. *Elife* 2: e00329, 2013.

Soukas AA, Kane EA, Carr CE, Melo JA, Ruvkun G. Rictor/TORC2 regulates fat metabolism, feeding, growth, and life span in *Caenorhabditis elegans*. *Genes Dev* 23: 496–511, 2009.

Steger KA, Avery L. The GAR-3 muscarinic receptor cooperates with calcium signals to regulate muscle contraction in the *Caenorhabditis elegans* pharynx. *Genetics* 167: 633–643, 2004.

Steger KA, Shtonda BB, Thacker CM, Snutch TP, Avery L. The *C. elegans* T-type calcium channel CCA-1 boosts neuromuscular transmission. *J Exp Biol* 208: 2191–2203, 2005.

Stirman JN, Crane MM, Husson SJ, Wabnig S, Schultheis C, Gottschalk A, Lu H. Real-time multimodal optical control of neurons and muscles in freely behaving *Caenorhabditis elegans*. *Nat Methods* 8: 153–158, 2011.

Tononi G, Sporns O, Edelman GM. Measures of degeneracy and redundancy in biological networks. *Proc Natl Acad Sci USA* 96: 3257–3262, 1999.

Touroutine D, Fox RM, Von Stetina SE, Burdina A, Miller DM 3rd, Richmond JE. *acr-16* encodes an essential subunit of the levamisole-resistant nicotinic receptor at the *Caenorhabditis elegans* neuromuscular junction. *J Biol Chem* 280: 27013–27021, 2005.

Waschuk SA, Bezerra AG, Shi L, Brown LS. *Leptosphaeria rhodopsin*: bacteriorhodopsin-like proton pump from a eukaryote. *Proc Natl Acad Sci USA* 102: 6879–6883, 2005.

You YJ, Kim J, Cobb MH, Avery L. Starvation activates MAP kinase through the muscarinic acetylcholine pathway in *Caenorhabditis elegans* pharynx. *Cell Metab* 3: 237–245, 2006.

You YJ, Kim J, Raizen DM, Avery L. Insulin, cGMP, and TGF-β signals regulate food intake and quiescence in *C. elegans*: a model for satiety. *Cell Metab* 7: 249–257, 2008.

Zhang F, Aravanis AM, Adamantidis A, de Lecea L, Deisseroth K. Circuit-breakers: optical technologies for probing neural signals and systems. *Nat Rev Neurosci* 8: 577–581, 2007.

Zhang YC, Baldwin JG. Ultrastructure of the post-corpus of *Zeldia punctata* (Cephalobina) for analysis of the evolutionary framework of nematodes related to *Caenorhabditis elegans* (Rhabditina). *Proc Biol Sci* 267: 1229–1238, 2000.